Towards Improved Acetylcholinesterase Inhibitors: A Structural and Computational Approach

X. Barril[1], M. Orozco [2*] and F. J. Luque [1*]

[1] *Departament de Fisicoquímica. Facultat de Farmàcia. Universitat de Barcelona. Avgda. Diagonal s/n. Barcelona 08028. Spain;* [2] *Departament de Bioquímica i Biologia Molecular. Facultat de Química. Universitat de Barcelona. c/. Martí Franqués 1. 08028 Barcelona. Spain*

Abstract: During the last years, solving the X-ray crystallographic structure of both the unliganded acetylcholinesterase (AChE) and AChE complexes with various inhibitors has provided valuable knowledge of the interactions that mediate inhibitor binding. This structural information allows us to rationalize differences in binding affinities for related analogues, and more importantly opens new strategies to design compounds with improved pharmacological properties. This is illustrated in the case of the recently reported huprines, which are a new class of very potent and selective acetylcholinesterase inhibitors.

INTRODUCTION

Alzheimer's disease (AD) is the fourth leading cause of death in people over 65 years old in western industrialized countries [1]. Only in the United States 4 million people are estimated to be afflicted with the disease, and the number is expected to increase to 14 million by the middle of the 21st century. Given the overwhelming damage caused by AD not only in the patients, but also to their families, and the increasing cost required for health assistance, it is imperative to seek effective measures for combating this disease, which is becoming one of the major health problems.

The cholinergic hypotesis is still the most successful approach for the symptomatic treatment of AD. This hypothesis postulates that at least some of the cognitive decline experienced by AD patients results from a deficiency in acetylcholine and thus in cholinergic neurotransmission. Therefore, inhibition of acetylcholinesterase (AChE) appears to be a natural therapeutic strategy to palliate the cognitive deficit in AD. At present there is a large amount of information concerning the crystallographic structure of acetylcholinesterase (AChE) as well as of various AChE-inhibitor complexes. Based on this information, computational methods and molecular modeling studies can be intensively used to gain insight into the mechanism of action of the enzyme and the molecular determinants that modulate the inhibitory potency of inhibitors. In turn, this knowledge can be exploited to design new compounds leading to more effective therapeutic strategies. This manuscript reviews recent developments in these areas, paying particular attention to the design of huprines, a new class of very potent and selective acetylcholinesterase (AChE) inhibitors.

*Address correspondence to this author at the Departament de Fisicoquímica. Facultat de Farmàcia. Universitat de Barcelona. Avgda. Diagonal s/n. Barcelona 08028. Spain; Fax: +34 93 403 5987; E-mail: javier@far1.far.ub.es or M. Orozco: :modesto@luz.bq.ub.es

ALZHEIMER'S DISEASE

The definitive causes of AD have not yet been fully elucidated, though the multifactorial origin of the pathogenesis of AD is clearly established [2]. Genetic studies have identified pathogenic mutations in a number of genes that include apolipoprotein E allele ε4, presenillin-1 and presenillin-2, and the β-amyloid precursor protein genes. All of the presenillin mutations analyzed so far increase the levels of secreted β-amyloid peptide [3], whose deposition in the brain is an early and critical feature of AD, thus supporting a central role for β-amyloid in the pathogenesis of AD.

β-amyloid (Aβ) peptide is the main component of the senile plaques and fibrillary tangles that constitute one of the neurohistopathological features of AD. Formation of the Aβ peptide requires proteolytic cleavage of a large transmembrane protein, the β-amyloid precursor protein, which is constitutively expressed in many cell types. An overproduction of the Aβ peptide and its subsequent deposition as insoluble amyloid plaques may represent the key pathological event that triggers the disease. Accordingly, the Aβ protein has become a primary target in the development of effective therapies, including β- and γ-secretase inhibitors to supress Aβ production, Aβ aggregation inhibitors, Aβ deposit dissolving agents, and immunization with Aβ peptide. Current NMR [4-8] and molecular modeling [9-11] studies are being conducted to unravel the structure and dynamics of the Aβ peptide and to understand the molecular basis of the amyloid fibryl formation.

The basic approach for the treatment of the early symptoms of AD for the past 20 years has been, nevertheless, the replacement of several deficient neutransmitters [12-15]. This therapeutic approach relies on the so-called cholinergic hypothesis of cognitive disfunction, which relates the cognitive decline experienced by AD patients to the deficiency in the neurotransmitter acetylcholine (ACh) in central nervous system. This

1389-5575/01 $20.00+.00

hypothesis is supported by the fact that cholinergic neurons are markedly damaged in AD patient brains. Cholinergic neurotransmission can be enhanced by drugs acting at the pre-synaptic level (choline precursors, ACh releasers, presynaptic muscarinic autoreceptor antagonists) and at the post-synaptic level (muscarinic and nicotinic agonists). However, the only drugs currently approved for the treatment of the cognitive deficit in AD act at the synaptic level by inhibiting AChE, which leads to a decay in the hydrolysis of the neutrotransmitter ACh and accordingly an increase in the bioavailability of ACh at the synaptic cleft, thus improving cholinergic neurotransmission.

It has been shown that AChE consistently colocalizes with the amyloid deposits characteristics of AD [16]. Recent studies have identified that AChE enhances the aggregation of Aβ peptide fragments comprising residues 12-28 and 25-35, but has no effect on the fragment with residues 1-16 [16]. These results, together with binding assays, have suggested that AChE may contribute to the generation of amyloid deposits and/or physically affects fibril assembly. Moreover, it has also been shown that the neurotoxicity of Aβ peptide aggregates depends on the amount of AChE bound to the complexes, suggesting that AChE may play a key role in the neurodegeneration observed in AD brain [17]. These evidences have stimulated the identification of AChE regions related to noncholinergic functions of the enzyme, such as adhesion and Aβ deposition [18]. It is not clear, nevertheless, that this feature of AChE in AD patients might be modulated by AChE inhibitors.

ACETYLCHOLINESTERASE ENZYME

Cholinesterases [19] constitute a family of enzymes that fall broadly into two types depending on their substrate specificity. Those enzymes that preferentially hydrolyse acetylesters such as ACh are called acetylcholinesterases or acetylcholine acetylhydrolases (EC 3.1.1.7), and those that hydrolise other types of esters such as butyrylcholine are termed butyrylcholinesterases (BChE) or acylcholine acylhydrolases (EC 3.1.1.8). The main function of AChE is the rapid hydrolysis of the neurotransmitter ACh at the cholinergic synapses. The hydrolysis reaction proceeds by nucleophilic attack to the carbonyl carbon, acylating the enzyme and liberating choline. This is followed by a rapid hydrolysis of the acylated enzyme yielding acetic acid, and the restoration of the enzyme. Because BChE does not have known specific natural substrates, its physiological function is less clear and might be involved in the detoxification of natural compounds.

The 3D structure of *Torpedo californica* AChE was initially solved at 2.8 Å resolution [20], and later refined to 2.5 Å resolution [21]. The enzyme monomer (Fig. **1**) is an α/β protein that contains 537 amino acids. It consists of 12-stranded mixed β sheet surrounded by 14 α helices. The most remarkable feature of the protein is a deep and narrow gorge, i. e. the active site gorge, around 20 Å long, that penetrates halfway into the enzyme and widens out close to its base. Fourteen highly conserved aromatic residues line a substantial portion of the surface of the gorge. The active site is unusual because it contains Glu, not Asp, in the Ser-His-acid catalytic (Ser200-His440-Glu327) triad and because the relation of the triad to the rest of the protein approximates a mirror image to that seen in serine proteases. Two other Glu residues (Glu199 and Glu327) are key for orienting the imidazole of His440 according to the steric and electrostatic features of the ligand bound to Ser200 [22,23]. Experimental and theoretical-suggest that Glu199 also stabilizes the transition state for the formation of tehtrahedral intermediate in the acylation step [24,25]. Another interesting structural feature is that the putative "anionic" site that binds the quaternary moiety of choline corresponds to a tryptophan (Trp84) residue. This unexpected finding, nevertheless, has received further support from theoretical considerations that reveal the large stability of cation-π complexes [26-28]. In addition to the active site, a second binding site, i. e. the "peripheral anionic" site, has also been identified and assigned to Trp279. Recent studies point out that the peripheral site acts as an initial binding site for substrate entry to the acylation site, thus accelerating the hydrolysis of acetylcholine at low substrate concentration [29]. Other authors have suggested that the peripheral site might modulate cation clearance and product release [30].

The long and narrow active site gorge seems inconsistent with the enzyme's high catalytic rate, as underlined by the large value of the k_{cat}/K_m, which is ~10^9 $M^{-1}.s^{-1}$ (this value is somewhat lower at physiological ionic strengths) [31,32]. This striking catalytic efficiency has stimulated the theoretical study of the kinetics of ligand binding to AChE. Calculations show the presence of a strong electrostatic field that directs cations into the active site gorge and have established a direct relationship between the electrostatic potential within the active site and the rate enhancement for substrate binding [33-37]. Owing to the fact that such electrostatic fields appear to be steady and strong, substrate molecules that encounter these attractive fields experience a continuous pull toward the active site [38], hindering the diffusion of the substrate out of the active site. The role of specific charged residues in the electrostatic attraction of ligands has been extensively studied [39-41], and Asp72 has been suggested to play a particularly important role in trapping the ligand within the gorge. Another interesting aspect is the proposal of conformation gating as a mechanism for enzyme specificity of AChE [42]. Such a gate would involve the aromatic rings of Tyr121, Phe290, Phe330, Phe331, and Tyr334, and the reorientation of these residues would temporarily make way for the incoming substrate. This mechanism would then allow the enzyme to achieve enzyme specificity by dynamic modulation of the active site accessibility.

Finally, molecular dynamics simulations show the occurrence of transient opening of short channels, large enough for a water molecule to pass, through a thin wall of the active site near Trp84 [43-45]. This finding suggests that substrate, products, or solvent could move through this "back door", in addition to the entrance revealed by the crystallographic structure. Electrostatic calculations show a strong field at the back door, oriented to attract the substrate and the reaction product, choline, and to repel the other reaction product, acetate. Alternative pathways for release of reaction products have also been examined [46]. Neverthe-

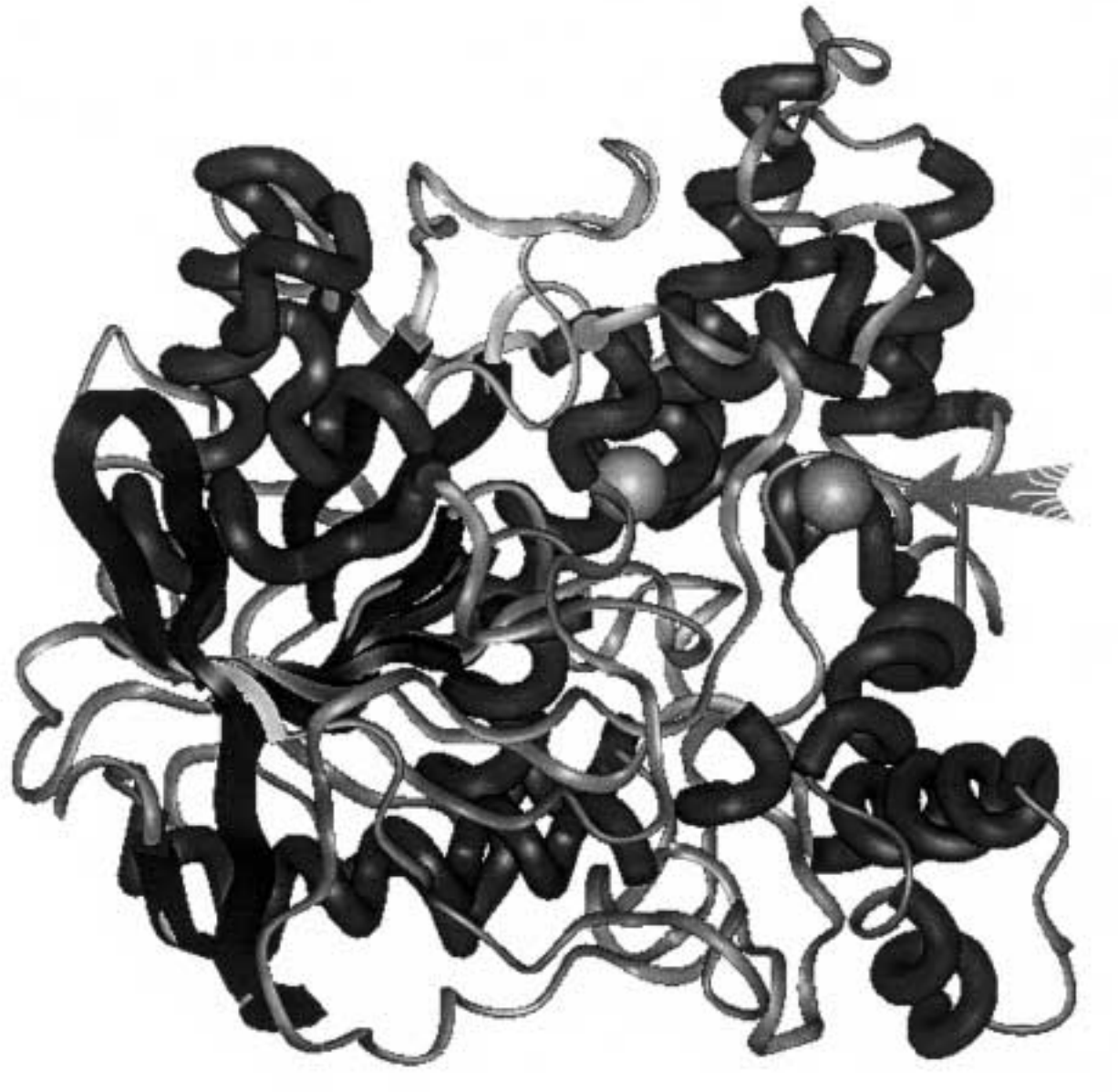

Fig. (1). 3D structure of the *Torpedo californica* AChE. The entry to the gorge is indicated by the arrow. The spheres indicate the location of the peripheral grey (dark) and active white (light) sites.

less, there is not yet experimental evidence supporting the functional role of the back door hypothesis.

ACHE INHIBITORS

The first drug approved by the FDA for the treatment of AD senile dementia was tacrine (Cognex®; Fig. **2**) [47,48]. Owing to the fact that tacrine exhibits severe side effects, efforts have been conducted to develop tacrine-related analogues with improved pharmacological properties, like amiridine (NIK-247), which is under clinical evaluation [49], and different tetracyclic derivatives [50-52]. Efforts have also been focused in developing other drugs with the pharmacological profile of AChE inhibitors (see Fig. **2**), such as rivastigmine (Exelon®) [50] and donepezil (Aricept®) [53]. The former is a miotine derivative that inhibits the enzyme by pseudoirreversible carbamoylation of the serine residue of the catalytic triad. Donepezil is an *N*-benzylpiperidine derivative that inhibits reversibly AChE. Recent efforts have led to the development of several compounds whose efficacy is under clinical evaluation, such as the physostigmine-derivative eptastigmine [55] and the donepezil-derivatives TAK-147 [56] and CP-118,954 [57], as well as other carbamoyloxy derivatives [58,59]. Other inhibitors are metrifonate (Nivalin®) [60,61], and minaprine-derivatives

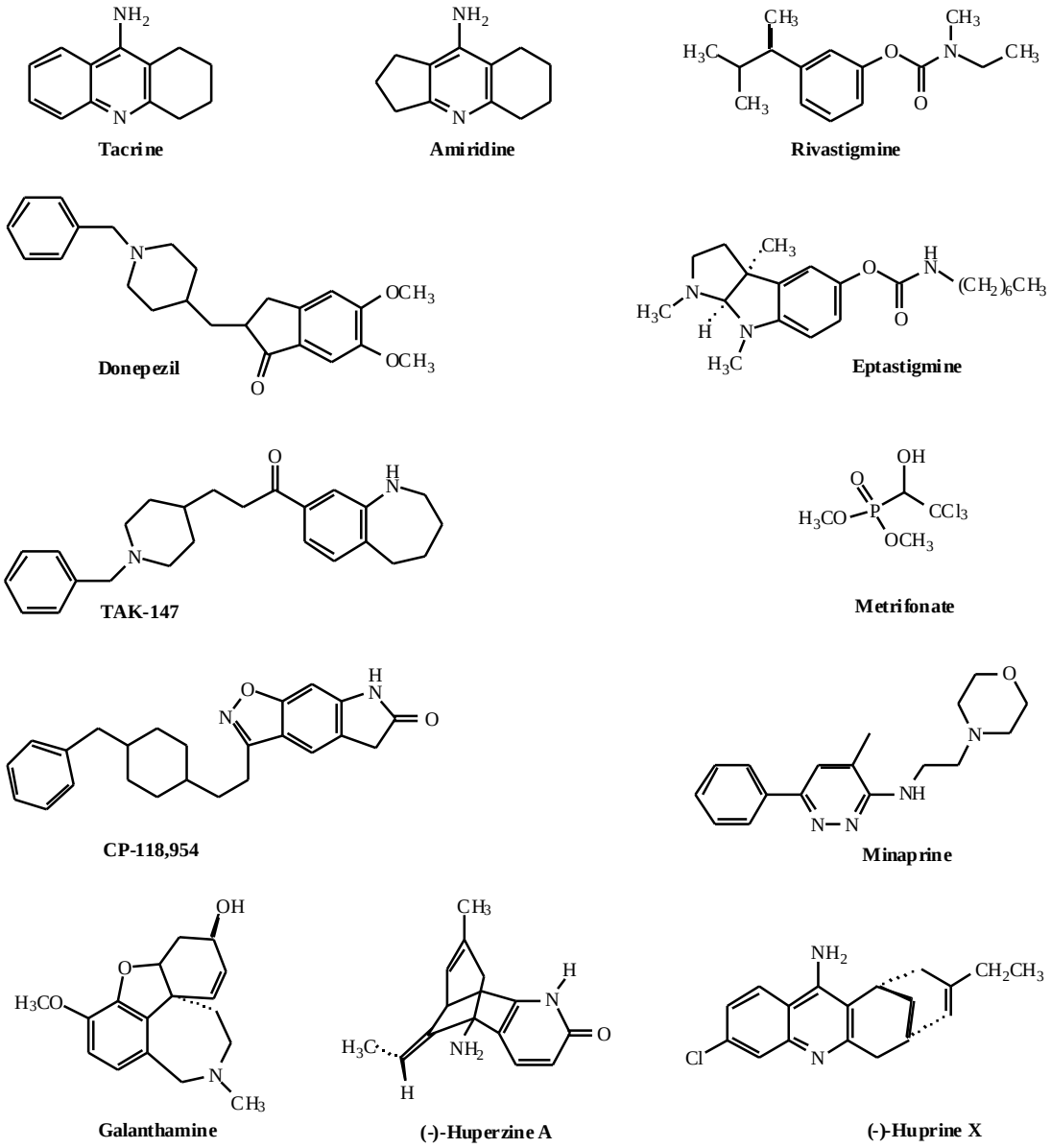

Fig. (2). Schematic representation of diverse AChE inhibitors.

[62]. Other strategies rely on the use of compounds of natural origin, such as galanthamine (Reminyl®) [63,64] and (-)-huperzine A [65,66], which has been marketed as a dietary supplement in USA.

A recent strategy to develop new AChE inhibitors consist in the association of structural fragments of the same or different drugs. At this point, an interesting approach is the design of compounds able to interact simultaneously with both the catalytic and peripheral sites of AChE. The general structure includes two components separated by a spacer group (normally an oligomethylene unit) with a suitable length. This is the case of a series of homo and heterodimeric tacrine-based inhibitors [67-69], where different basic amines of differing hydrophobicity were chosen as peripheral site ligands. The homodimeric bis-tacrine analogue is 149-fold more potent as AChE inhibitor than tacrine, and near 100-fold more selective for AChE than for BChE [67,69]. The optimum huperzine A-tacrine dimeric derivative is 13-fold more potent than (-)-huperzine A, and 25-fold more potent than tacrine [68]. Other studies have examined the inhibitory potencies of heterodimeric derivatives of huperzine A [70] and galanthamine [71], which were between 2 and 5-fold more potent than tacrine. Novel imidazole-based [72] and polyamine-based [73] inhibitors able to interact simultaneously with both catalytic and peripheral sites have also been examined in recent studies.

A somewhat different approach is based on the mixing of two different substructures pertaining to AChE inhibitors that bind the enzyme in proximal regions of the binding pocket. These compounds are designed to retain the basic pharmacophoric features of the two parent compounds, thus enhancing mutually their inhibitory effects. This is the

guideline adopted in the development of huprines [74], which were conceived as hybrid compounds between the 4-aminoquinoline unit of tacrine and the carbobicyclic unit of huperzine A (see below). The most potent compound, named huprine X, binds human AChE with an inhibition constant of 26 pM [75], which is one of the highest affinities yet reported. Under equivalent assay conditions, this affinity is 180 times that of (-)-huperzine A, 1200 times that of tacrine, and 40 times that of donepezil.

CRYSTALLOGRAPHIC STUDIES

Knowledge of the 3D structure of the complexes between AChE and inhibitors provides a rational basis for structure-related drug design aimed at developing synthetic analogues with improved therapeutic properties. Table **1** reports a selection of the currently available AChE-inhibitor complexes in the Protein Data Bank [76]. Some inhibitors bind nearby the binding pocket that encloses the catalytic

Table 1. Crystallographic Structures of the Unliganded AChE and its Complexes with Various Inhibitors Available in the Protein Data Bank

	Code	Resolution	Enzyme source	Reference
AChE	2ACE	2.5	Torpedo californica	21
	1EA5	1.8	Torpedo californica	NA [a]
	1QO9	2.72	Drosophila	101
	2CLJ	----	Human (homology-built model)	
Bw284C51	1E3Q	2.85	Torpedo californica	NA
Decamethonium	1ACL	2.8	Torpedo californica	80
	1MAA	2.9	Mouse	83
Edrophonium	2ACK	2.4	Torpedo californica	80
(-)-Huperzina A	1VOT	2.5	Torpedo californica	21
Donepezil	1EVE	2.5	Torpedo californica	81
Fasciculin-II	1FSS	3.0	Torpedo californica	102
	1MAH	3.2	Mouse	103
	1B41	2.8	Human	23
	1F8U	2.7	Human (E202Q mutant)	23
Galanthamine	1QTI	2.5	Torpedo californica	104
	1DX6	2.3	Torpedo californica	105
Tacrine and Tacrine-Related Derivatives	1ACJ	2.8	Torpedo californica	80
	1QON	2.7	Drosophila	101
	1DX4	2.7	Drosophila	101
Covalently-Bound Inhibitors				
	2DFP	2.3	Torpedo californica	79
	1VXR	2.2	Torpedo californica	22
	1SOM	2.2	Torpedo californica	79

[a] Not yet published.

machinery, whereas others are placed along the active gorge that connects the catalytic and peripheral sites. In one case (fasciculin-II) there is a direct interaction with the peripheral binding site. There are also a number of structures that involve covalently bound inhibitors, which have proved to be valuable for gaining insight into the mechanism of action of the enzyme as well as in its ageing [22,77-79].

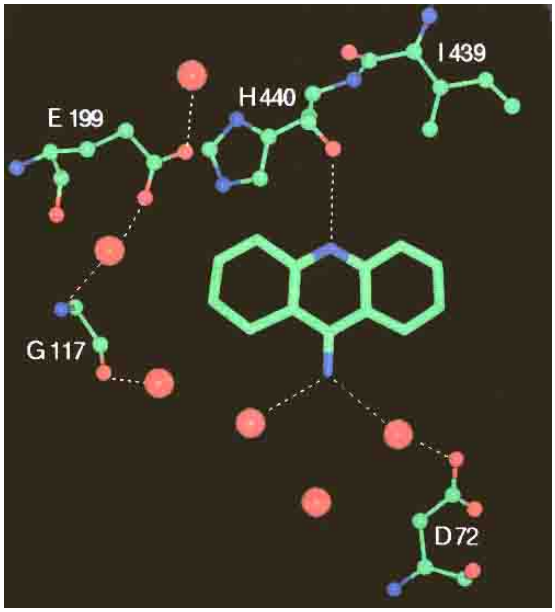

Fig. (3). Detail of the 3D structure of AChE complex with tacrine. Large red spheres represent the oxygen atoms of water molecules. Hydrogen-bonds are shown by dashed lines.

Several studies have pointed out that, in spite of this chemical diversity, the global 3D structure of the enzyme is very well preserved in all cases [23,80-82]. However, local structural deformations, mainly in loop regions, have been observed in some cases [23,82]. For instance, comparison of the fasciculin-II complexes of human, mouse and *Torpedo californica* AChE reveals that the only noticeable difference in their 3D structures is located in the 312-317 loop of the enzyme [23, 83]. Another example is the flipped peptide bond between residues Gly117 and Gly118 in the AChE complex with (-)-huperzine A compared to the native enzyme [21], which might presumably contribute to the slow binding of this inhibitor.

The chemical differences between inhibitors enlighten the diversity and complexity of the network of interactions between the inhibitor and the enzyme. For the purposes of this review, particular attention is paid to the analysis of the most relevant structural features that mediate ligand-enzyme binding for selected complexes. Harel *et al*. reported a detailed comparison of the 3D crystallographic structures of AChE complexes with tacrine, decamethonium, and edrophonium [80]. In the tacrine-AChE complex (Fig. **3**), tacrine is stacked against Trp-84, the ring nitrogen is hydrogen-bonded to the main-chain carbonyl oxygen of His440, and the amino nitrogen forms a hydrogen bond to a water molecule. In the decamethonium-AChE complex, the inhibitor is oriented along the narrow gorge leading to the active site. One quaternary group is opposed to the indole ring of Trp84 (at the active site), and the other one to that of Trp279 (near the top of the gorge). Finally, in the complex with edrophonium, the quaternary nitrogen of the ligand interacts with the indole of Trp84, and its *m*-hydroxyl displays bifurcated hydrogen bonding to two members of the catalytic triad, Ser200 and His440. Comparison of the 3D structures shows that the only remarkable conformational difference lies in the orientation of the phenyl ring of Phe330: while it lies parallel to the methylene chain of decamethonium, the phenyl ring contacts the ethyl substituent of edrophonium and stacks against the quinoline ring of tacrine.

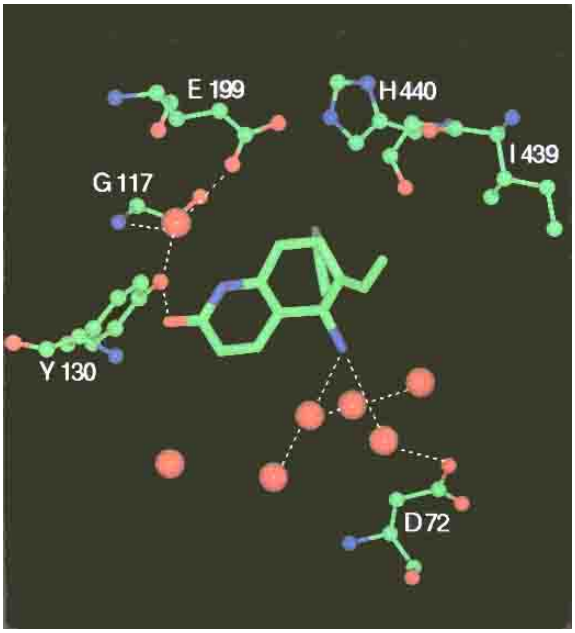

Fig. (4). Detail of the 3D structure of the AChE complex with (-)-huperzine A. Large red spheres represent the oxygen atoms of water molecules. Hydrogen-bonds are shown by dashed lines.

Solving the structure of the AChE complex with (-)-huperzine A (Fig. **4**) [21] revealed an unexpected binding mode compared to the orientation of ACh in the active site [20,84-87]. The amino group of this inhibitor forms an interaction with the aromatic rings of Trp84 and Phe330. The conformation of this latter residue is, nevertheless, different to that found in the complex with tacrine. There is also a hydrogen bond between the carbonyl group of the ligand with the hydroxyl oxygen of Tyr130, an unusually short contact between the ethylidene methyl group and the main oxygen of His440. Finally, there are several water molecules

linking the inhibitor to different residues in the binding pocket.

It is also interesting to examine the structural details of the binding of donepezil (E2020) to AChE (Fig. **5**) [81]. The first remarkable feature is that donepezil, which binds to AChE in the nanomolar range [13,87], adopts a unique orientation along the active site gorge extending from the anionic subsite of the active site to the peripheral site through aromatic interactions with conserved aromatic amino acid residues (Fig. **5**). The benzyl ring interacts through π−πstacking with the indole ring of Trp84, thus occupying the binding site for quaternary ligands. The charged nitrogen of the piperidine ring makes a cation-π interaction with the phenyl ring of Phe330, whose orientation is similar to that seen in the complex with decamethonium [80]. Finally, the indanone ring stacks against the indole ring of Trp279. Interestingly, all three structural units of E2020 forms discrete water-mediated contacts that seem to be crucial for binding and specificity.

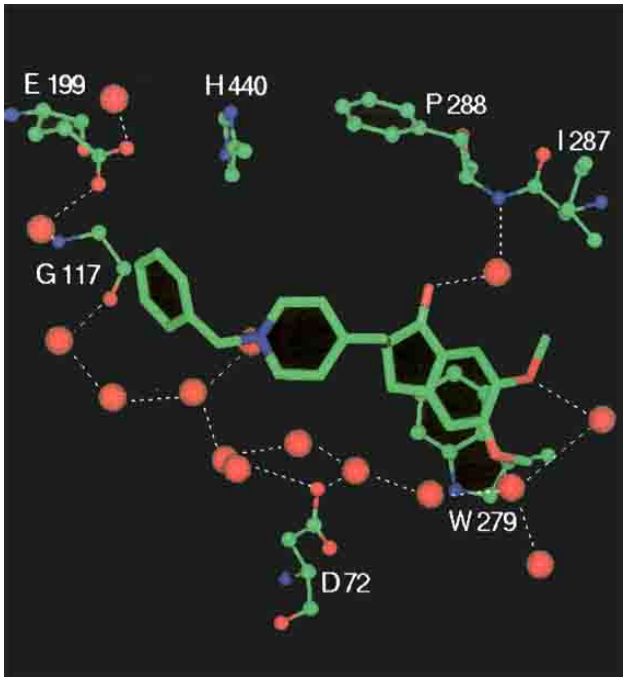

Fig. (5). Detail of the 3D structure of the AChE complex with donepezil. Large red spheres represent the oxygen atoms of water molecules. Hydrogen-bonds are shown by dashed lines.

The preceding analysis suffices to illustrate the importance of aromatic residues as binding sites in AChE. This structural feature is not only important for rational drug design, but might also suggest an *aromatic guidance* mechanism providing an array of low-affinity binding sites, thus enabling the rapid diffusion of ACh through the gorge down to the active site [20]. Another interesting point to be considered in the design of AChE inhibitors is the conformational flexibility of Phe330. In fact, comparison of different 3D structures permits to assign three main conformations to the phenyl ring of Phe330 [81]. First, the orientation in the native enzyme or in the complexes with (-)-huperzine A and edrophonium (χ1 ~ -170 degrees). Second, the conformation found in the complex with tacrine (χ1 ~ 160 degrees). Third, the orientation observed in complexes with donepezil and decamethonium (χ1 ~ 125 degrees). A proper orientation of the side chain of this residue is then key for ligand recognition. Moreover, site-directed mutagenesis studies have shown that elimination of this residue has a significant effect on the k_{cat} of the enzyme [88,89], suggesting that Phe330 also modulates the catalytic efficacy of the enzyme. Finally, it is also worth noting the essential role played by water molecules in modulating the interaction of ligands with the enzyme. Even for bulky inhibitors such as donepezil, there are still a large number of water molecules in the gorge. Many of the conserved water molecules can be assumed to be an integral part of the gorge, which must be considered for a proper understanding of both ligand binding and ligand traffic inside the enzyme [87].

HUPRINES: A NEW CLASS OF ACHE INHIBITORS

Huprines are a new class of AChE inhibitors that were conceived as hybrids between tacrine and (-)-huperzine A (Fig. **4**) [74]. In fact, they combine the 4-aminoquinoline unit of tacrine and the carbobicyclic unit of (-)-huperzine A (Fig. **6**). As noted above, the underlying assumption was that the heterocyclic rings of both tacrine and (-)-huperzine A might occupy proximal regions in the active site of AChE, and subsequently the hybrid should exhibit increased inhibitory potency relative to the parent compounds.

The first huprine derived from the synthetic conjuctive approach mentioned above, 12-amino-6,7,10,11-tetrahydro-9-methyl-7,11-methanocycloocta[*b*]quinoline (compound **1** in Table **2**), turned out to be an AChE inhibitor 2-fold more potent than tacrine and slightly more potent than (-)-huperzine A. Based on these results, this compound was used as a lead for structure-activity relationship studies [74], including modifications of the benzene ring of the 4-aminoquinoline unit, the methylene bridge between positions 7 and 11, and the three carbon unsaturated bridge between positions 7 and 11. Subsequent studies led to the synthesis of huprine X (compound **7** in Table **2**; see also Fig. **2**), a tight-binding reversible inhibitor of AChE, which has one of the highest affinities yet reported (see Table **2**), as noted in its binding to human AChE with an inhibition constant of 26 pM [74].

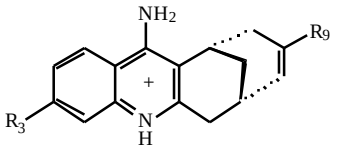

Fig. (6). Schematic representation of the (-)-enantiomer of the huprine.

Table 2. Pharmacological Data of Selected Derivatives of (-)-Huprines[a], (-)-Huperzine A and Tacrine

Compound	R_3	R_9	IC_{50}(human)	IC_{50}(bovine)
1	H	CH_3	47.1 ± 6.3	n.d.
2	H	CH_2CH_3	27.4 ± 3.1	n.d.
3	F	CH_3	3.49 ± 0.84	n.d.
4	Cl	CH_3	1.15 ± 0.11	0.32 ± 0.10
5	F	CH_2CH_3	6.73 ± 0.95	2.11 ± 0.58
6	CH_3	CH_2CH_3	4.5 ± 0.8	n.d.
7	Cl	CH_2CH_3	1.30 ± 0.26	0.32 ± 0.09
(-)-Huperzine A			74.0 ± 5.5	260 ± 18
Tacrine			130 ± 10	205 ± 18

[a] IC_{50} inhibitory concentration (nM) of AChE from bovine and human erythrocytes. Data taken from refs. 94 and 100. (n.d.: not determined)

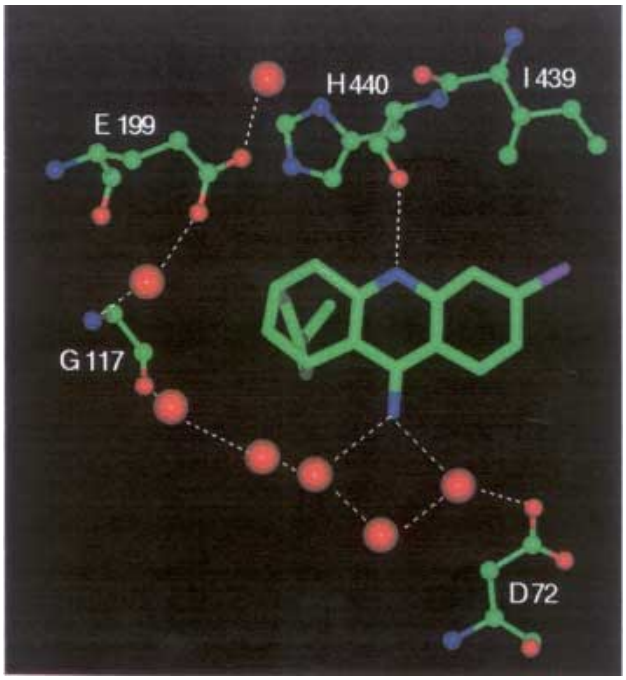

Fig. (7). Detail of the 3D structure of the AChE complex with (-)-huprine X derived from molecular modeling studies (refs. 94, 95 and 100). Large red spheres represent the oxygen atoms of water molecules. Hydrogen-bonds are shown by dashed lines.

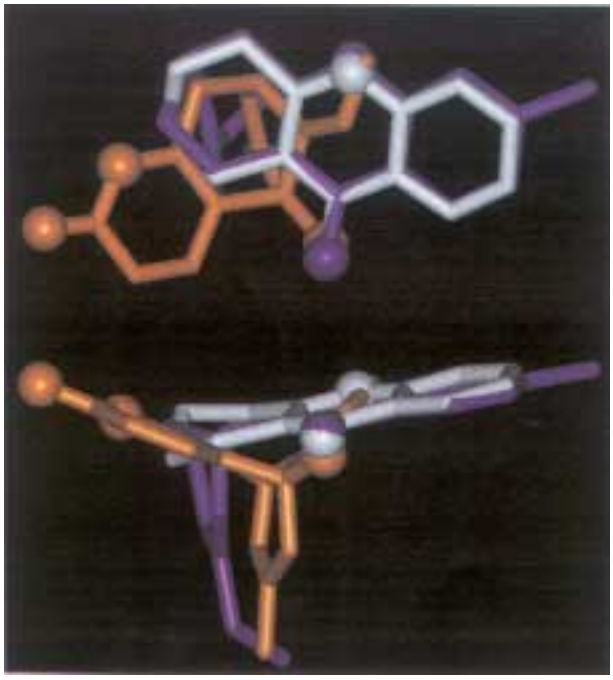

Fig. (8). Superimposition of the structure of (-)-huprine X (blue) in the putative binding mode to AChE and the structures of tacrine (white) and (-)-huperzine A (orange) in their crystallographic complexes with AChE. The two views are related by a 180 degree rotation about the long axis of the molecules.

X-ray diffraction analysis revealed the absolute configuration of the most active (levorotatory) enantiomer of huprines, which is opposite to that of (-)-huperzine A [92]. Taking advantage of this information, as well as of the X-ray

3D structures of the AChE complexes with tacrine [80] and (-)-huperzine A [21], molecular modelling studies combined with CMIP calculations [93] and molecular dynamics

simulations were performed to differentiate between diverse binding modes that mimicked the basic features of the interaction of either tacrine or (-)-huperzine A with AChE [94,95]. As a result, a putative binding mode for the recognition of huprines in the active site of AChE was suggested, it being characterized by the following structural features (Fig. **7**): a) the quinoline ring is stacked between the indole ring of Trp84 and the phenyl ring of Phe330; b) the amino group occupies a position similar to that of the amino group in tacrine and the protonated amino group in (-)-huperzine A; the amino group is well hydrated, and it forms water-mediated contacts to residues such as Asp72 and Ser122; c) the ring NH group is hydrogen-bonded to the carbonyl oxygen of His440; and 4) the bicyclo[3.3.1]nonadiene unit of the (-)-enantiomer fits into a hydrophobic pocket formed by residues Tyr121, Phe290, Phe330 and Phe331.

It is worth noting that, according to the proposed binding model, huprines can be considered to be truly structural hybrids of tacrine and (-)-huperzine A (Fig. **8**), as far as the 4-aminoquinoline of huprines occupies the same position of the corresponding unit of tacrine, and the carbobicyclic unit of huprine is placed in a region close to the position occupied by the corresponding substructure of (-)-huperzine A, a fact that is only permitted when the levorotatory enantiomers of both huprine and huperzine A are considered.

The close structural resemblance between (-)-huprine, tacrine, and (-)-huperzine A suggests that attachment of substituents to equivalent positions of (-)-huprine and tacrine/(-)-huperzine A should lead to analogous changes in inhibitory potency. This is confirmed by the available experimental data. For instance, attachment of a fluorine atom at position 3 of tacrine increases the activity by a factor of 2.5 [96], and the same substitution in (-)-huprine leads to around 7-fold increase in the inhibitory potency (compounds **3** and **5** in Table **2**). An analogous effect is observed upon attachment of chlorine at position 3 (compounds **4** and **7** in Table **2**) of (-)-huprine, and at the equivalent position in tacrine and 1,4-methylenetacrine [97], and in dihydroquinazoline-based AChE inhibitors [98]. Concerning the structural similarity between (-)-huprine and (-)-huperzine A, replacement of methyl by phenyl in (-)-huperzine A is known to decrease the inhibitory activity by at least 1000-fold [99]. Replacement of methyl by ethyl in (-)-huprine slightly increases the inhibitory potency (see Table **2**), but bulkier substituents gives rise to a decrease in the binding affinity [94,100].

Detailed understanding between structure and inhibitory potency can be gained from molecular dynamics simulations combined to free energy calculations [95,100]. Calculations showed that the pattern of interactions between a series of substituted (-)-huprines and the enzyme (see above) was fully preserved along the simulation, thus supporting the stability of the proposed binding mode. In addition, free energy calculations allowed us to predict successfully the changes in inhibitory potency. Particularly, the increased binding affinity obtained upon chlorination at position 3 can be partly explained from the fact that the chlorine atom fills a hydrophobic cavity formed by residues Met436, Ile439 and Trp432 [100]. Similarly, free energy calculations also allows us to explain the slight increase in binding affinity observed upon replacement of methyl by ethyl at position 9 in terms of a better desolvation of the inhibitor [100].

CONCLUDING REMARKS

Though the definitive validation of the binding model has necessarily to await the X-ray 3D structure determination of the complex, the development of huprines illustrates how the available structural information can be exploited to establish a relationship between chemical structure and inhibitory potency. The wealth of structural information currently available should be valuable in developing compounds that effectively fill voids in the active site or that link the active and peripheral sites. Combined with *state-of-the-art* computational approaches, the increasing number of X-ray structures, involving inhibitors of diverse chemical complexity, as well as different binding sites and interaction patterns, constitutes then a very useful guidance to gain deeper understanding in the mechanism of action of the enzyme, and to design new compounds with improved pharmacological profile.

ACKNOWLEDGMENTS

We thank Dr. P. Camps and Dr. D. Muñoz-Torrero for valuable suggestions. We also acknowledge the Dirección General de Investigación Científica y Técnica (grants PB98-1222 and PM99-0046) and the Fundació La Marató-TV3 (project 3004/97) for financial support. X.B. is fellowship from the Spanish Ministerio de Educación y Cultura.

ABBREVIATIONS

AD = Alzheimer's disease

Aβ = β-amyloid peptide

ACh = Acetylcholine

AChE = Acetylcholinesterase

BChE = Butirylcholinesterase

CMIP = Classical molecular interaction potential

REFERENCES

[1] Boyd, B. *Drug News Perspect.*, **2000**, *13*, 425.

[2] Launer, L.J.; Frantiglioni, L.; Andersen, K.; Breteler, M.M.B.; Copeland, R.J.M.; Dartigues, J.F.; Lobo, A.; Martínez-Lage, J.; Soininen, H.; Hofman, A. In *Alzheimer's Disease and Related Disorders: Etiology, Pathogenesis and Therapeutics*. Iqbal, K.; Swaab, D.F.; Winblad, B.; Wisniewski, H.M. Eds. Wiley: New York, **1999**, pp. 9-15.

[3] Haas, C.; Selkoe, D. J. *Nature*., **1998**, *391*, 339.

[4] Balbach, J.J.; Ishii, Y.; Antzutkin, O.N.; Leapman, R.D.; Rizzo, N.W.; Dyda, F.; Reed, J.; Tycko, R. *Biochemistry*, **2000**, *39*, 13748.

[5] Zhang, S.; Iwata, K.; Lachenman, M.J.; Peng, J.W.; Li, S.; Stimson, E.R.; Lu, Y.A.; Felix, A.M.; Maggio, J.E.; Lee, J.P. *J. Struct. Biol*., **2000**, *130*, 130.

[6] Marcinowski, K.J.; Shao, H.; Clancy, E.L.; Zagorski, M.G. *J. Am. Chem. Soc*., **1998**, *120*, 11082.

[7] Coles, M.; Bicknell, W.; Watson, A.A.; Pairlie, D.P.; Craik, D.J. *Biochemistry*, **1998**, *37*, 11064.

[8] Shao, H.; Jao, S.C.; Ma, K.; Zagorski, M.G. *J. Mol. Biol*., **1999**, *285*, 755.

[9] George, A.R.; Howlett, D.R. *Biopolymers*, **1999**, *50*, 733.

[10] Massi, F.; Peng, J. W.; Lee, J. P.; Straub, J. E. *Biophys. J*., **2001**, *80*, 31.

[11] Massi, F.; Straub, J. *Proteins*, **2001**, *42*, 217.

[12] Gualtieri, F.; Deu, S.; Manetti, D.; Romanelli, M.N. *Farmacologie*, **1995**, *50*, 489.

[13] Brufani, M.; Filocamo, L.; Lappa, S.; Maggi, A. *Drugs Fut.*, **1997**, *22*, 397.

[14] Parnetti, L.; Senin, U.; Mecocci, P. *Drugs Fut*., **1997**, *53*, 752.

[15] Giacobini, E. *Jpn. J. Pharmacol*., **1997**, *74*, 225.

[16] Alvarez, A.; Opazo, C.; Alarcon, R.; Garrido, J.; Inestrosa, N.C. *J. Mol. Biol.*, **1997**, *272*, 348.

[17] Muñoz, F.J.; Inestrosa, N.C. *FEBS Lett.*, **1999**, *450*, 205.

[18] Johnson, G.; Moore, S. W. *Biochem. Biophys. Res. Comm.*, **1999**, *258*, 758.

[19] *Cholinesterases: Structure, Function, Mechanism, Genetics and Cell Biology*. Massoulié, J.; Bacou, F.; Barnard, E.; Chatonnet, A.; Doctor, B.P.; Quinn, D.M., Eds. American Chemical Society: Washington, **1991**.

[20] Sussman, J.L.; Harel, M.; Frolow, F.; Oefner, C.; Goldman, A.; Toker, L.; Silman, I. *Science*, **1991**, *253*, 872.

[21] Raves, M.L.; Harel, M.; Pang, Y.P.; Silman, I.; Kozikowski, A.P.; Sussman, J.L. *Nature Struct. Biol*., **1997**, *4*, 57.

[22] Millard, C.B.; Koellner, G.; Ordentlich, A.; Shafferman, A.; Silman, I.; Sussman, J.L. *J. Am. Chem. Soc.*, **1999**, *121*, 9883.

[23] Kryger, G.; Harel, M.; Giles, K.; Toker, L.; Velan, B.; Lazar, A.; Kronman, C.; Barak, D.; Ariel, N.; Shafferman, A.; Silman, I.; Sussman, J.L. *Acta Cryst.*, **2000**, *D56*, 1385.

[24] Radic, Z.; Gibney, G.; Kawamoto, S.; MacPhee-Quigley, K.; Bongiorno, C.; Taylor, P. *Biochemistry*, **1992**, *31*, 9760.

[25] Wlodek, S. T.; Antosiewicz, J.; Briggs, J. M. *J. Am. Chem. Soc*. **1997**, *119*, 8159.

[26] Ma, J.C.; Dougherty, D.A. *Chem. Rev.*, **1997**, *97*, 1303

[27] Cubero, E.; Luque, F.J.; Orozco, M. *Proc. Natl. Acad. Sci., USA* **1998**, *95*, 5976.

[28] Gallivan, J.P.; Dougherty, D.A. *Proc. Natl. Acad. Sci. USA*, **1999**, *96*, 9459.

[29] Szegletes, T.; Mallender, W.D.; Thomas, P.J.; Rosenberry, T.L. *Biochemistry*, **1999**,*38*,122.

[30] Van Belle, D.; De Maria, L.; Iurcu, G.; Wodak, S.J. *J. Mol. Biol*., **2000**, *298*, 705.

[31] Nolte, H.J.; Rosenberry, T.L.; Neumann, E. *Biochemistry*, **1980**, *19*, 3705.

[32] Pryor, A.N.; Selwood, T.; Leu, L.S.; Andracki, M.A.; Lee, B.H.; Rao, M.; Rosenberry, R.; Doctor, B.P.; Silman, I.; Quinn, D.M. *J. Am. Chem. Soc*., **1992**, *114*, 3896.

[33] Ripoll, D.R.; Faerman, C.H.; Axelsen, P.H.; Silman, I.; Sussman, J.L. *Proc. Natl. Acad. Sci. USA*, **1993**, *90*, 5128.

[34] Tan, R.C.; Truong, T.N.; McCammon, J.A.; Sussman, J.L. *Biochemistry*, **1993**, *32*, 401

[35] Antosiewicz, J.; McCammon, J.A.; Gilson, M.K. *Biochemistry*, **1996**, *35*, 7819.

[36] Antosiewicz, J.; Briggs, J.M.; Elcock, A.H.; Gilson, M.K.; McCammon, J.A. *J. Comput. Chem.*, **1996**, *17*, 1633.

[37] Zhou, H.X.; Briggs, J.M.; McCammon, J.A. *J. Am. Chem. Soc*., **1996**, *118*, 13069.

[38] Wlodek, S.T.; Shen, T.; McCammon, J.A. *Biopolymers*, **2000**, *53*, 265.

[39] Tara, S.; Elcock, A.H.; Kirchhoff, P.D.; Briggs, J.M.; Radic, Z.; Taylor, P.; McCammon, J. A. *Biopolymers*, **1998**, *46*, 465.

[40] Radic, Z.; Kirchhoff, P.D.; Quinn, D.M.; McCammon, J.A.; Taylor, P. *J. Biol. Chem*., **1997**, *272*, 23265.

[41] Antosiewicz, J.; Wlodek, S.T.; McCammon, J.A. *Biopolymers*, **1996**, *39*, 85.

[42] Zhou, H. X.; Wlodek, S. T.; McCammon, J. A. *Proc. Natl. Acad. Sci. USA*, **1998**, *95*, 9280.

[43] Gilson, M.K.; Straatsma, T.P.; McCammon, J.A.; Ripoll, D.R.; Faerman, C.H.; Axelsen, P.H.; Silman, I.; Sussman, J.L. *Science*, **1994**, *263*, 1276.

[44] Fareman, C.; Ripoll, D.; Bon, S.; Le Feuvre, Y.; Morel, N.; Massoulié, J.; Sussman, J.L.; Silman, I. *FEBS Lett*., **1996**, *386*, 65.

[45] Tara, S.; Straatsma, T. P.; McCammon, J. A. *Biopolymers*, **1999**, *50*, 35.

[46] Enyedy, I.J.; Kovach, I.M.; Brooks, B.R. *J. Am. Chem. Soc*., **1998**, *120*, 8043.

[47] *Tacrine*. *Drugs Fut*., **1987**, *12*, 1032.

[48] Davis, K.L.; Powchick, P. *Lancet*, **1995**, *345*, 625.

[49] *NIK-247*. *Drugs Fut*., **1994**, *19*, 343

[50] McKenna, M.T.; Proctor, G.R.; Young, L.C.; Harvey, A.L. *J. Med. Chem*., **1997**, *40*, 3516.

[51] Recanatini, M.; Cavalli, A.; Belluti, F.; Piazzi, L.; Rampa, A.; Bisi, A.; Gobbi, S.; Valenti, P.; Andrisano, V.; Bartolini, M.; Cavrini, V. *J. Med. Chem*., **2000**, *43*, 2007.

[52] Rampa, A.; Bisi, A.; Belluti, F.; Gobbi, S.; Valenti, P.; Andrisano, V.; Cavrini, V.; Cavalli, A.; Recanatini, M. *Bioorg. Med. Chem*., **2000**, *8*, 497.

[53] *SDZ-ENA-713*. *Drugs Fut*., **1994**,*19*, 656.

[54] Sugimoto, H.; Yamanishi, Y.; Iimura, Y.; Kawakami, Y. *Curr. Med. Chem*., **2000**, *7*, 303.

[55] McCleland, K.J.; Benfield, P. *CNS Drugs*, **1988**, *9*, 69.

[56] *TAK-147. Drugs Fut*., **1995**, *20*, 248.

[57] Villalobos, A.; Butler, T. W.; Chapin, D. S.; Chen, Y.L.; DeMattos, S.B.; Ives, J. L.; Jones, S.B.; Liston, D.R.; Nagel, A.A.; Nason, D.M.; Nielsen, J.A.; Ramirez, A.D.; Shalaby, I.A.; White, W.F. *J. Med. Chem*., **1998**, *35*, 2802.

[58] Valenti, P.; Rampa, A.; Bisi, A.; Fabbri, G.; Andrisano, V.; Cavrini, V. *Med. Chem. Res*., **1995**, *5*, 255.

[59] Rampa, A.; Bisi, A.; Valenti, P.; Recanatini, M.; Cavalli, A.; Andrisano, V.; Cavrini, V.; Fin, L.; Buriani, A.; Giusti, P. *J. Med. Chem*., **1998**, *41*, 3976.

[60] Cummings, J.L.; Cyrus, P.A.; Biever, F.; Mas, J.; Orazem, J.; Gulanski, B. *Neurology*, **1998**, *50*, 1214

[61] Morris, J.C.; Cyrus, P.A.; Orazem, J.; Biever, F.; Ruzicka, B.B.; Gulanski, B. *Neurology*, **1998**, *50*, 1222.

[62] Contreras, J.M.; Rival, Y.M.; Chayer, S.; Bourguignon, J.J.; Wermuth, C.G. *J. Med. Chem*., **1999**,*42*, 730.

[63] Bores, G.M.; Kosley, R.W. *Drugs Fut*., **1996**, *21*, 621.

[64] Rainer, M. *CNS Drugs*, **1997**, *7*, 89.

[65] Kozikowski, A.P.; Tückmantel, W. *Acc. Chem. Res.*, **1999**, *32*, 641.

[66] Bai, D.L.; Tang, X.C.; He, X.C. *Curr. Med. Chem*., **2000**, *7*, 355.

[67] Carlier, P.R.; Chow, E.S.H.; Han, Y.; Liu, J.; El Yazal, J.; Pang, Y.P. *J. Med. Chem*., **1999**, *42*, 4225.

[68] Carlier, P.R.; Du, D.M.; Han, Y.; Liu, J.; Pang, Y.P. *Bioorg. Med. Chem. Lett*., **1999**, *9*, 2335.

[69] Carlier, P.R.; Han, Y.F.; Chow, E.S.H.; Li, C.P.L.; Wang, H.; Lieu, T.X.; Wong, H.S.; Pang, Y.P. *Bioorg. Med. Chem*., **1999**, *7*, 351.

[70] Carlier, P.R.; Du, D.M.; Han, Y.F.; Liu, J.; Perola, E.; Williams, I.D.; Pang, Y.P. *Angew. Chem., Int. Ed*., **2000**, *39*, 1775.

[71] Guillou, C.; Mary, A.; Renko, D.Z.; Gras, E.; Thal, C. *Bioorg. Med. Chem. Lett*. **2000**, *10*, 637.

[72] Castro, A.; Richards, W.G.; Lyne, P.D. *Med. Chem. Res*., **1999**, *9*, 98.

[73] Melchiorre, C.; Andrisano, V.; Bolognesi, M.L.; Budriesi, R.; Cavalli, A.; Cavrini, V.; Rosini, M.; Tumiatti, V.; Recanatini, M. *J. Med. Chem*., **1988**, **41**, 4186.

[74] Camps, P.; Muñoz-Torrero, D. *Mini Rev. Med. Chem*., **2001**, in press.

[75] Camps P.; Cusack, B.; Mallender, W.D.; El Achab, R.; Morral, J.; Muñoz-Torrero, D.; Rosenberry, T.L. *Mol. Pharmacol*., **2000**, *57*, 409.

[76] Berstein, F.C.; Koetzle, T.F.; Williams, G.J.B.; Meyer, E.F., Jr.; Brice, M.D.; Rodgers, J.R.; Kennard, O. *J. Mol. Biol*., **1977**, *112*, 535.

[77] Shafferman, A.; Ordenlitch, A.; Barak, D.; Stein, D.; Ariel, N.; Velan, B. *Biochem. J*., **1996**, *318*, 833.

[78] Ordenlitch, A.; Barak, D.; Kronman, C.; Benschop, H.P.; De Jong, L.P.A.; Ariel, N.; Barak, R.; Segall, Y.; Velan, B.; Shafferman, A. *Biochemistry*, **1999**, *38*, 3055.

[79] Millard, C.B.; Kryger, G.; Ordenlitch, A.; Greenblatt, H.M.; Harel, M.; Raves, M.L.; Segall, Y.; Barak, D.; Shafferman, A.; Silman, I.; Sussman, J.L. *Biochemistry*, **1999**, *38*, 7032.

[80] Harel, M.; Schalk, I.; Ehret-Sabatier, L.; Bouet, F.; Goeldner, M.; Hirth, C.; Axelsen, P.H.; Silman, I.; Sussman, J.L. *Proc. Natl. Acad. Sci. USA*, **1993**, *90*, 9031.

[81] Kryger, G.; Silman, I.; Sussman, J.L. *Structure*, **1999**, *7*, 297.

[82] Boutonnet, N.; Van Belle, D.; Wodak, S.J. *Theor. Chem. Acc*., **2001**, *112*, 10.

[83] Bourne, Y.; Taylor, P.; Bougis, P.E.; Marchot, P. *J. Biol. Chem*., **1999**, *274*, 2963.

[84] Pang, Y.P.; Kozikowski, A. P. *J. Comput. Aided Mol. Design*, **1994**, *8*, 669.

[85] Ashani, Y.; Grunwald, J.; Kronman, C.; Velan, B.; Shafferman, A. *Mol. Pharmacol*., **1994**, *45*, 555.

[86] Saxena, A.; Qian, N.; Kovach, I.M.; Kozikowski, A.P.; Pang, Y.P.; Vellom, D.C.; Radic, Z.; Quinn, D.; Taylor, P.; Doctor, B.P. *Prot. Sci*., **1994**, *3*, 1770.

[87] Galli, A.; Mori, F.; Benini, L.; Cacciarelli, N. *Eur. J. Pharmacol.*, **1994**, *270*, 189.

[88] Ordenlitch, A.; Barak, D.; Kronman, C.; Flashner, Y.; Leitner, M.; Segall, Y.; Ariel, N.; Cohen, S.; Velan, B.; Shafferman, A. *J. Biol. Chem.*, **1993**, *268*, 17083.

[89] Radic, Z.; Pickering, N.A.; Vellom, D.C.; Camp, S.; Taylor, P. *Biochemistry*, **1993**, *32*, 12074.

[90] Koellner, G.; Kryger, G.; Millard, C.B.; Silman, I.; Sussman, J.L.; Steiner, T. *J. Mol. Biol*., **2000**, *296*, 713.

[91] Badia, A.; Baños, J.E.; Camps, P.; Contreras, J.; Görbig, D.M.; Muñoz-Torrero, D.; Simon, M.; Vivas, N.M. *Bioorg. Med. Chem.*, **1998**, *6*, 427.

[92] Camps, P.; Contreras, J.; Font-Badia, M.; Morral, J.; Muñoz-Torrero, D.; Solans, X. *Tetrahedron: Asymmetry*, **1998**, *9*, 835.

[93] Gelpi, J.L.; Kalko, S.; Barril, X.; Cirera, J.; De la Cruz, X.; Luque, F.J.; Orozco, M. CMIP program. *Proteins*, **2001**, In Press.

[94] Camps, P.; El Achab, R.; Görbig, D.M.; Morral, J.; Muñoz-Torrero, D.; Badia, A.; Baños, J.E.; Vivas, N.M.; Barril, X.; Orozco, M.; Luque, F.J. *J. Med. Chem.*, **1999**, *42*, 3227.

[95] Barril, X.; Orozco, M.; Luque, F.J. *J. Med. Chem.*, **1999**, *42*, 5110.

[96] Kawakami, H.; Ohuchi, R.; Kitano, M.; Ono, K. Patent EPO 0 268 871 A1. Sumimoto Pharmaceuticals Co., Ltd., **1987**.

[97] Gregor, V.E.; Emmerling, M.R.; Lee, C.; Moore, C.J. *Bioorg. Med. Chem. Lett.*, **1992**, *2*, 861.

[98] Jaen, J.C.; Gregor, V.E.; Lee, C.; Davis, R.; Emmerling, M. *Bioorg. Med. Chem. Lett.*, **1996**, *6*, 737.

[99] Kozikowski, A.P.; Xia, Y.; Reddy, E.R.; Tückmantel, W.; Hanin, I.; Tang, X.C. *J. Org. Chem.*, **1991**, *56*, 4636.

[100] Camps, P.; El Achab, R.; Görbig, D.M.; Morral, J.; Muñoz-Torrero, D.; Badia, A.; Baños, J.E.; Vivas, N.M.; Barril, X.; Orozco, M.; Luque, F.J. *J. Med. Chem.*, **2000**, *43*, 4657.

[101] Harel, M.; Kryger, G.; Rosenberry, T.L.; Mallender, W.D.; Lewis, T.; Fletcher, R.J.; Guss, J.M.; Silman, I.; Sussman, J.L. *Prot. Sci.*, **2000**, *9*, 1063.

[102] Harel, M.; Kleywegt, G.J.; Ravelli, R.B.G.; Silman, I.; Sussman, J.L. *Structure*, **1995**, *3*, 1355.

[103] Harel, M.; Quinn, D.M.; Nair, H.K.; Silman, I.; Sussman, J.L. *J. Am. Chem. Soc*., **1996**, *118*, 2340.

[104] Bartolucci, C.; Perola, E.; Pilger, C.; Fels, G.; Lamba, D. *Proteins* **2001**, *42*, 182.

[105] Greenblatt, H.M.; Kryger, G.; Lewis, T.; Silman, I.; Sussman, J.L. *Febs. Lett.*, **1999**, *463*, 321.